JOURNAL OF AGRICULTURAL AND FOOD CHEMISTRY

Kinetics of Mushroom Tyrosinase Inhibition by Quercetin

QING-XI CHEN† AND ISAO KUBO*

Department of Environmental Science, Policy and Management, University of California, Berkeley, California 94720-3112

The effects of quercetin on the activity of mushroom tyrosinase were studied. The equilibrium constants for this inhibitor binding with the enzyme molecule were established. The inhibition mechanism obtained from Lineweaver−Burk plots show that quercetin is a competitive inhibitor. In the time course of the oxidation of L-3,4-dihydroxyphenylalanine (L-DOPA) catalyzed by the enzyme in the presence of different concentrations of quercetin, the rate decreased with increasing time until a straight line was approached. The inhibition of tyrosinase by quercetin is a slow and reversible reaction with residual enzyme activity. The microscopic rate constants were determined for the reaction of quercetin with the enzyme.

KEYWORDS: Tyrosinase inhibitory activity; quercetin; kinetics; competitive inhibition

INTRODUCTION

Tyrosinase (EC 1.14.18.1), also known as polyphenol oxidase (PPO) (*1*−*4*), is a copper containing mixed-function oxidase widely distributed in microorganisms, animals, and plants. This oxidase catalyzes two distinct reactions of melanin synthesis, the hydroxylation of a monophenol (monophenolase activity) and the conversion of an *o*-diphenol to the corresponding *o*-quinone (diphenolase activity), and is involved in the formation of pigments such as melanins (*5*). The hydroxylation of L-tyrosine, the initial step in melanin synthesis, is also the initial step in catecholamine synthesis. The enzymatic oxidation of L-tyrosine to melanin is of considerable importance because melanin has many functions, and alterations in melanin synthesis occur in many disease states. For example, melanoma-specific anticarcinogenic activity is linked with tyrosinase activity (*6*). Melanin pigments are also found in the mammalian brain. Tyrosinase may play a role in neuromelanin formation in the human brain, particularly in the substantia nigra. This mixed-function oxidase could be central to dopamine neurotoxicity and may contribute to the neurodegeneration associated with Parkinson's disease (*7*). Tyrosinase inhibitors have become increasingly important in medicinal (*8*) and cosmetic (*9*) products, primarily in relation to hyperpigmentation.

In our previous paper, the characterization of quercetin (**1**) (see **Figure 1** for structures) was shown to be the principal tyrosinase inhibitor present in the dried flower of *Heterotheca inuloides* CASS (Compositae), and the fresh flower of *Trixis michuacana* var *longifolia* (D. Dow) C. Anderson (Compositae). Both are known as "arnica" in Mexico and are used as medicinal plants. Quercetin was shown to inhibit the enzymatic oxidation of L-DOPA by chelating copper in the enzyme. The chelation mechanism seems to be specific to flavonols as long as the 3-hydroxyl group is free (*10*, *11*). From a practical point of view, copper chelators are currently targeted because they possess no oxidizable hydroxyl group, and, more importantly, the binuclear copper active site is common in all the tyrosinase, regardless of their sources. Comparing IC_{50} values, quercetin is the most potent tyrosinase inhibitor among the flavonoids characterized (*10*, *11*). Although the great potential of flavonols as tyrosinase inhibitors has been demonstrated, their kinetic behavior has been little explored. The aim of the present experiment is, therefore, to carry out a kinetic study of the inhibition of the *o*-diphenolase (catecholase) activity of mushroom tyrosinase by flavonols and to evaluate the kinetic parameters and constants characterizing the system. Hence, the kinetics of tyrosinase inhibition by quercetin was studied in detail.

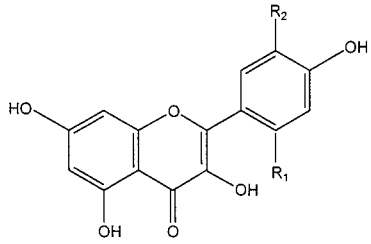

1. R_1 = H; R_2 = OH
2. R_1 = H; R_2 = H
3. R_1 = OH; R_2 = H

Figure 1. Chemical structure of quercetin and related compounds.

MATERIALS AND METHODS

Chemicals. Quercetin, kaempferol, and morin were available from our previous work (*10*, *11*). Dimethyl sulfoxide (DMSO) and L-DOPA were purchased from Sigma Chemical Co. (St. Louis, MO).

* To whom correspondence should be addressed. Phone: (510) 643-6303. Fax: (510) 643-0215. E-mail: ikubo@uclink4.berkeley.edu.
† Present address: The Key Laboratory of Ministry of Education for Cell Biology and Tumor Cell Engineering, Xiamen University, Xiamen 361005, People's Republic of China.

10.1021/jf011378z CCC: $22.00
Published on Web 06/06/2002

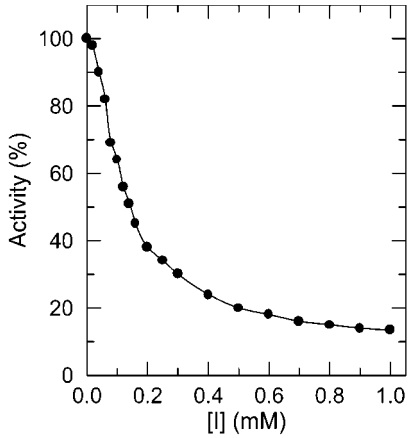

Figure 2. Effects of quercetin on the activity of mushroom tyrosinase for the catalysis of L-DOPA (enzyme concentration 4.0 μg/mL).

Enzyme Assay. The mushroom tyrosinase (EC 1.14.18.1) used for the bioassay was purchased from Sigma. The following conditions were used for the present experiment. First, mushroom tyrosinase differs from other sources to some degree (*12*), but this fungal source was used because of its ready availability. Second, mode of inhibition is known to depend on the structure of both the substrate and inhibitor, so L-DOPA was used as the substrate, unless otherwise specified. Therefore, the activity studied is with respect to *o*-diphenolase inhibitory activity of mushroom tyrosinase. Third, tyrosinase is known to catalyze a reaction between two substrates, a phenolic compound (L-DOPA) and oxygen, but the assay was carried out in air-saturated aqueous solutions. Therefore, Michaelis constant (K_m) and maximum velocity (V_m) values determined in these conditions were only apparent, and the effect of oxygen concentration on these parameters is unknown.

Enzyme activity was determined at 30 °C by following the increase in absorbance at 475 nm (ϵ = 3700 M^{-1} cm^{-1}) accompanying the oxidation of the substrate (L-DOPA). One unit (U) of enzymatic activity was defined as the amount of enzyme increasing 0.001 absorbance at 475 nm in this condition. The progress-of-substrate-reaction theory previously described (*13*) was applied to the current study of the inhibition kinetics of mushroom tyrosinase by quercetin. In this method, the mushroom tyrosinase (1.0 mg/mL in 0.1 M phosphate buffer pH 6.8) was first diluted with water at 50 times, and then 50 μL of the solution was added to 200 μL of an assay substrate solution with 25 μL DMSO containing different concentrations of quercetin. The substrate reaction progress curve was analyzed to obtain the reaction rate constants. The reaction was carried out under a constant temperature of 30 °C. Absorption measurements were recorded using a Spectra MAX plus Microplate spectrophotometer. The kinetic and inhibition constants were obtained by the method previously described (*14*−*17*).

RESULTS AND DISCUSSION

Effect of Quercetin on the Activity of Mushroom Tyrosinase. The effect of quercetin on the oxidation of L-DOPA by mushroom tyrosinase was studied first. Inhibition of the enzyme by quercetin was concentration-dependent as shown in **Figure 2**. As the concentrations of quercetin increased, the residual enzyme activity was rapidly decreased, but it was not completely suppressed. The inhibitor concentration leading to 50% activity lost (IC_{50}) was estimated to be 0.13 mM.

Figure 3 shows that in the presence of different concentrations of quercetin the enzyme activity was dependent on the enzyme concentration. The plots of the residual enzyme activity versus the concentrations of enzyme at different concentrations of quercetin gave a family of straight lines (**Figure 3**) which passed through the origin, indicating that the inhibition of the enzyme by quercetin was reversible. Increasing the quercetin concentration resulted in the descending of the slopes of the lines.

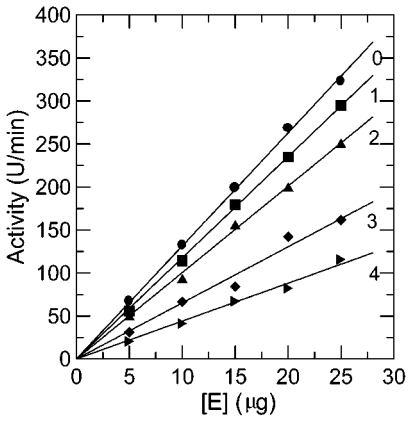

Figure 3. Relationship of the catalytic activity of mushroom tyrosinase with the enzyme concentrations at different concentrations of quercetin. Concentrations of quercetin for curves 0–4 were 0, 10, 20, 30, and 40 μM, respectively.

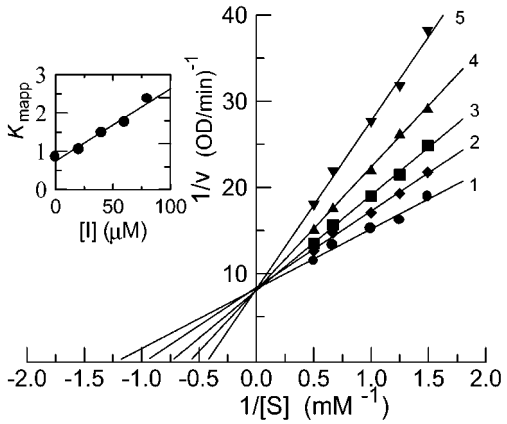

Figure 4. Lineweaver–Burk plots for inhibition of quercetin on mushroom tyrosinase for the catalysis of DOPA at 30 °C, pH 6.8. Concentrations of quercetin for curves 1–5 were 0, 20, 40, 60, and 80 μM, respectively; the enzyme concentration was 4.0 μg/mL. The inset represents the plot of K_{mapp} versus the quercetin concentration for determining the inhibition constants K_I.

Determination of the Inhibition Type of Quercetin on Mushroom Tyrosinase. The kinetic behavior of mushroom tyrosinase during the oxidation of L-DOPA was studied. Under the condition employed in the present investigation, the oxidation reaction of L-DOPA by mushroom tyrosinase follows Michaelis−Menten kinetics. The kinetic parameters for mushroom tyrosinase obtained from a Lineweaver−Burk plot (**Figure 4**, line 1) show that K_m is equal to 0.84 mM and V_{max} is equal to 122 U/min (33.0 μM/min). The results illustrated in **Figure 4** show that quercetin is a competitive inhibitor because increasing the quercetin concentration resulted in a family of lines with a common intercept on the $1/v$ axis but with different slopes. The equilibrium constant for inhibitor binding, K_I, was obtained from a plot of the apparent Michaelis−Menten constant (K_{mapp}) versus the concentration of quercetin, which is linear as shown in the inset. The obtained constant is 0.0386 mM, as summarized in **Table 1**.

Kinetics of the Substrate Reaction in the Presence of Different Concentrations of Quercetin. The time course of the oxidation of L-DOPA catalyzed by the enzyme in the presence of different quercetin concentrations is shown in **Figure 5a**. At each concentration of quercetin, the rate decreased with increasing time until a straight line was approached, the slope of which decreased with increasing quercetin concentra-

Table 1. Kinetics Parameters and Microscopic Inhibition Rate Constants of Mushroom Tyrosinase by Quercetin[a,b]

IC_{50}	0.13 mM
K_m	0.84 mM
V_m	122 U/min
inhibition	reversible
inhibition type	competitive
K_I	0.0386 mM
k_{+0}	0.0216 (mM^{-1} sec^{-1})[a]
	0.0219 (mM^{-1} sec^{-1})[b]
k_{-0}	0.832×10^{-3} (sec^{-1})[a]

[a] From plot of 1/*A* against [*S*]. [b] From plot *A*/*v* against 1/[*S*].

tion. The above results, as analyzed by Tsou's method (*13*), suggest that the formation of the inactive $E_{oxy}I$ complex is a slow and reversible reaction. This can be written as follows:

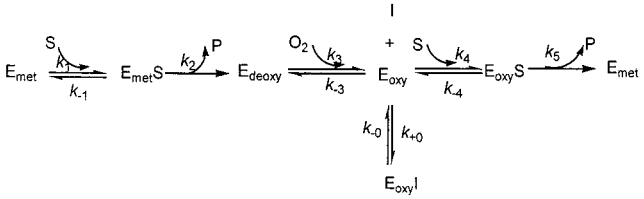

where *E* (E_{met}, E_{deoxy}, and E_{oxy}), *S*, *I*, and *P* denote enzyme (three forms of the enzyme), substrate, inhibitor (quercetin), and product, respectively; EI and ES are the respective compounds. As it is usually the case that $[S] \gg [E_0]$ and $[I] \gg [E_0]$, the product formation can be written as follows (*14*, *15*):

$$[P]_t = \frac{Bv}{A[I]+B}t + \frac{A[I]v}{(A[I]+B)^2} - \frac{A[I]}{(A[I]+B)^2}e^{-(A[I]+B)t} \quad (1)$$

$$A = \frac{k_{+0} \times K_m}{K_m + [S]} \quad (2)$$

$$B = k_{-0} \quad (3)$$

where $[P]_t$ is the concentration of the product formed at time *t*, which is the reaction time; *A* and *B* are the apparent rate constants for the forward and reverse reactions of inhibition, respectively; [*S*] and [*I*] are the concentrations of the substrate and inhibitor, respectively; *v* is the initial rate of reaction in the absence of the inhibitor, where $v = V_m[S]/(K_m + [S])$. When *t* is sufficiently large, the curves become straight lines and the product concentration is written as $[P]_{calc}$:

$$[P]_{calc} = \frac{Bv}{A[I]+B}t + \frac{A[I]v}{(A[I]+B)^2} \quad (4)$$

Combining eqs 1 and 4 yields

$$[P]_{calc} - [P]_t = \frac{A[I]v}{(A[I]+B)^2}e^{-(A[I]+B)t} \quad (5)$$

where $[P]_{calc}$ is the product concentration to be expected from the straight-line portions of the curves as calculated from eq 4, and $[P]_t$ is the product concentration actually observed at time *t*. Plots of $\ln([P]_{calc} - [P]_t)$ versus reaction time (*t*) give a series of straight lines at different concentrations of inhibitor ([*I*]) with slopes of $-(A[I] + B)$. A secondary plot of the slopes versus [*I*] gives a straight line. The apparent forward and reverse rate constants, *A* and *B*, can be obtained from the slope and intercept

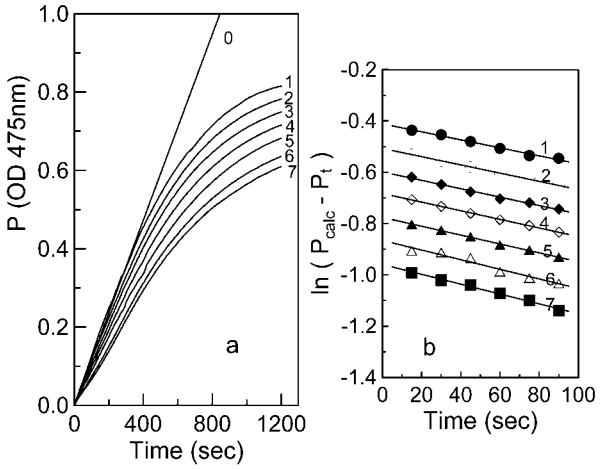

Figure 5. Course of the substrate reaction in the presence of different concentrations of quercetin. The final assay conditions: 250 μL system containing 0.05 M phosphate sodium buffer pH 6.8, 2.0 mM L-DOPA as substrate, and different concentrations of quercetin, 4.0 μg/mL mushroom tyrosinase, at 30 °C. (a) The time course of the substrate oxidation reaction. The concentrations of quercetin for curves 0–7 were 0, 20, 40, 60, 80, 100, 120, and 140 μg/mL, respectively. (b) Plots of $\ln([P]_{calc} - [P]_t)$ vs time. Data were taken from curves 1–7 in **Figure 1**.

of this straight line. The value of *B* directly gives the microscopic rate constant k_{-0}.

From eq 2, we can get

$$\frac{1}{A} = \frac{1}{k_{+0} \times K_m}[S] + \frac{1}{k_{+0}} \quad (6)$$

A plot of 1/*A* versus [*S*] gives a straight line with $1/(k_{+0} \times K_m)$ as the slope of the straight line and $1/k_{+0}$ as the intercept on the *y*-axis.

Combining eq 2 and the Michaelis−Menten equation gives

$$\frac{A}{v} = \frac{K_m \times k_{+0}}{V_m} \times \frac{1}{[S]} \quad (7)$$

A plot of *A*/*v* versus 1/[*S*] gives a straight line with K_m k_{+0}/V_{max} as the slope of the straight line, which passes through the origin, indicating that the quercetin is a competitive inhibitor of the enzyme (*15*, *17*). As K_m and V_{max} are known quantities from measurements of the substrate reaction in the absence of the modifier at different substrate concentrations, the rate constant k_{+0} can be easily determined. Plots of $\ln([P]_{calc} - [P]_t)$ versus *t* give a family of straight lines at different concentrations of quercetin with slopes of $-(A[I] + B)$, **Figure 5b**.

Kinetics of the Reaction at Different Substrate Concentrations in the Presence of Quercetin. Figure 6a shows the kinetic courses of the reaction at different L-DOPA concentrations in the presence of 60 μM of quercetin. It can be seen from **Figure 6a** that when *t* is sufficiently large, both the initial rate and the slope of the asymptote increase with increasing substrate concentration. Similarly, plots of $\ln([P]_{calc} - [P]_t)$ versus *t* give a family of straight lines at different concentrations of the substrate with slopes of $-(A[I] + B)$ as shown in **Figure 6b**. The apparent forward and reverse rate constants, *A* and *B*, can be obtained through suitable plots.

Determination of the Microscopic Rate Constants of Inhibition of Quercetin on the Enzyme. A plot of the slopes of the straight lines in **Figure 5b** versus quercetin concentration [*I*] gives the straight line, curve 5 in **Figure 7**. Similarly, data

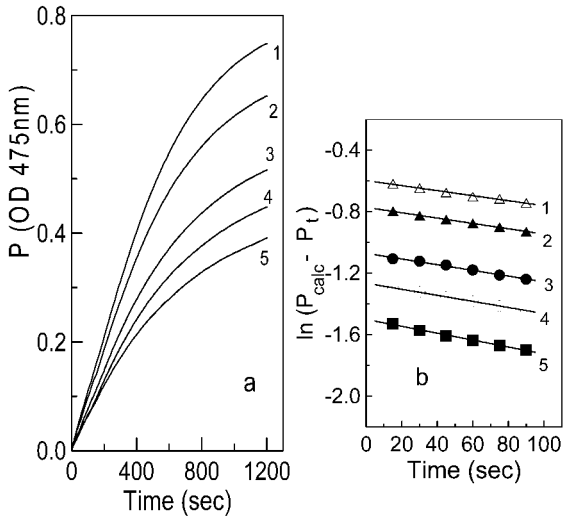

Figure 6. Course of the substrate reaction at different substrate concentrations in the presence of quercetin. Experimental conditions were the same as those for **Figure 4** except the L-DOPA concentrations were different. (a) The time course of the substrate oxidation reaction. The concentrations of L-DOPA for curves 1–5 were 2.0, 1.5, 1.0, 0.80, and 0.67 mM, respectively. (b) Plots of $\ln([P]_{calc} - [P]_t)$ vs time. Data were taken from curves 1–5 in (a).

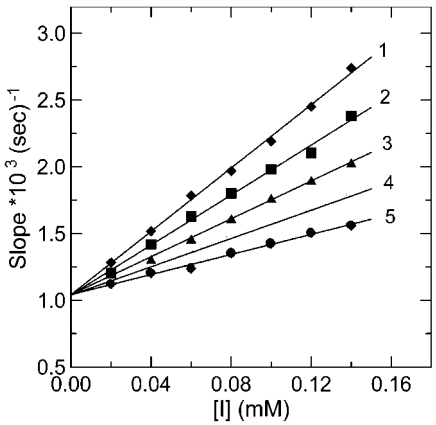

Figure 7. Secondary plots of the slopes versus the concentrations of quercetin ([*I*]) for a series of fixed substrate concentrations. Experimental conditions were the same as those for **Figure 4** except for the L-DOPA concentrations. The substrate concentrations for curves 1–5 were 0.67, 0.80, 1.0, 1.5, and 2.0 mM, respectively.

collected for other concentrations give the other straight lines in **Figure 7**. All the straight lines have a common intercept on the ordinate. The apparent reverse rate constant B can be obtained from the ordinate intercept. The value of B is then equal to the microscopic rate constant k_{-0} given in **Table 1**.

Figure 8 shows that the plot of $1/A$ versus [S] gives a straight line with $1/(k_{+0} \times K_m)$ as the slope of the line and $1/k_{+0}$ as the intercept on the y-axis. According to eq 6, from the slope and intercept, we can determine the microscopic rate constant k_{+0}. **Figure 9** shows that the plot of A/v versus $1/[S]$ gives a straight line that passes through the origin. According to eq 7, the slope of the straight line gives the value of $K_m k_{+0}/V_{max}$. The microscopic rate constant k_{+0} was then obtained from the slope (**Table 1**).

In summery, the results obtained by the current kinetic study are consistent with those of the previous reports. Noticeably, the tyrosinase inhibitory activity of flavonols such as quercetin, kaempferol (**2**), and morin (**3**) was previously described as

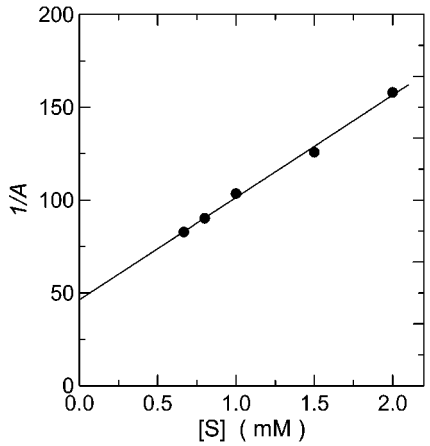

Figure 8. Plot of $1/A$ versus [S]. The values of A were obtained from the substrate reaction in the presence of quercetin.

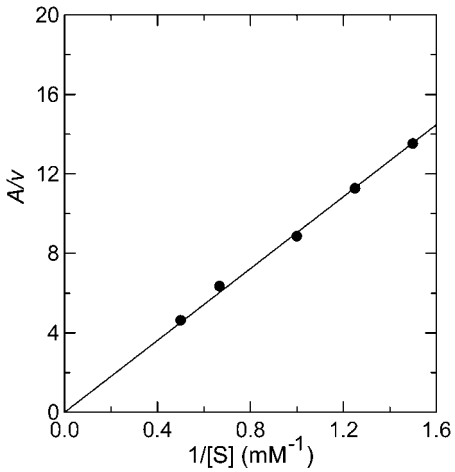

Figure 9. Plot of A/v vs $1/[S]$. The values of v and A were obtained from the substrate reaction in the absence of quercetin and from **Figure 6**.

coming from their ability to chelate one copper in the binuclear active center of the enzyme (*18*−*20*). Hence, flavonols inhibit the enzyme competitively, and hence, the inhibition mechanism is a classical competitive type. The inhibition of tyrosinase by flavonols is common as a slow and reversible reaction with remaining enzyme activity. As far as the inhibitory activity of tyrosinase is concerned, the pyrone moiety is responsible because the pyrone moiety preferentially chelates copper in the enzyme even if other moieties exist in the same molecule. This, however, does not rule out the possibility that the catechol moiety in quercetin is associated in part with this mechanism of inhibition. In this regard, quercetin showed the most potent inhibitory activity among the flavonols tested but the reason for this difference is still largely unknown. There still seems to be a lack of important knowledge for designing effective tyrosinase inhibitors.

Quercetin is characterized from many edible plants. Tyrosinase inhibitors isolated from the edible plants may be superior to nonnatural products. Despite this advantage, the biological significance of quercetin as a tyrosinase inhibitor in living systems is still largely unknown. The results so far obtained indicate that their further evaluation is needed, from not only one aspect, but from a whole and dynamic perspective.

ACKNOWLEDGMENT

We are grateful to M. Takasaki for providing us an authentic quercetin.

LITERATURE CITED

(1) Zawistowski, J.; Biliaderis, C. G.; Eskin, N. A. M. Polyphenol oxidase. In *Oxidative Enzymes in Foods*; Robinson, D. S., Eskin, N. A. M., Eds.; Elsevier: London, 1991; pp 217−273.

(2) Whitaker, J. R. In *Food Enzymes, Structure and Mechanism*; Wong, D. W. S., Ed.; Chapman & Hall: New York, 1995; pp 271−307.

(3) Sánchez-Ferrer, A.; Rodríguez-López, J. N.; García-Cánovas, F.; García-Carmona, F. Tyrosinase: A comprehensive review of its mechanism. *Biochim. Biophys. Acta* **1995**, *1247*, 1−11.

(4) Mayer, A. M.; Harel, E. Phenoloxidases and their significance in fruit and vegetables. In *Food Enzymology*; Fox, P. F., Ed.; Elsevier: London, 1998; pp 373−398.

(5) Robb, D. A. Tyrosinase. In *Copper Proteins and Copper Enzymes*; Lontie, R., Ed.; CRC Press: Boca Raton, FL, 1984; Vol. II, pp 207−240.

(6) Prezioso, J. A.; Epperly, M. W.; Wang, N.; Bloomer, W. D. Effects of tyrosinase activity on the cytotoxicity of 4-*S*-cysteaminylphenol and *N*-acetyl-4-*S*-cysteaminylphenol in melanoma cells. *Cancer Lett*. **1992**, *63*, 73−79.

(7) Xu, Y.; Stokes, A. H.; Freeman, W. M.; Kumer, S. C.; Vogt, B. A.; Vrana, K. E. Tyrosinase mRNA is expressed in human substantia nigra. *Mol. Brain Res*. **1997**, *45*, 159−162.

(8) Mosher, D. B.; Pathak, M. A.; Fitzpatrick, T. B. Vitiligo, etiology, pathogenesis, diagnosis, and treatment. In *Update: Dermatology in General Medicine*; Fitzpatrick, T. B., Eisen, A. Z., Wolff, K., Freedberg, I. M., Austen, K. F., Eds.; McGraw-Hill: New York, 1983; pp 205−225.

(9) Maeda, K.; Fukuda, M. *In vitro* effectiveness of several whitening cosmetic components in human melanocytes. *J. Soc. Cosmet. Chem*. **1991**, *42*, 361−368.

(10) Kubo, I.; Kinst-Hori, I.; Ishiguro, K.; Chaudhuri, S. K.; Sanchez, Y.; Ogura, T. Flavonols from *Heterotheca inuloides*. Tyrosinase inhibitory activity and structural criteria. *Bioorg. Med. Chem*. **2000**, *8*, 1585−1591.

(11) Kubo, I.; Kinst-Hori, I. Flavonols from saffron flower: Tyrosinase inhibitory activity and inhibition mechanisms. *J. Agric. Food Chem*. **1999**, *47*, 4121−4125.

(12) van Gelder, C. W. G.; Flurkey, W. H.; Wichers, H. J. Sequence and structural features of plant and fungal tyrosinases. *Phytochemistry* **1997**, *45*, 1309−1323.

(13) Tsou, C. L. Kinetics of substrate reaction during irreversible modification of enzyme activity. *Adv. Enzymol. Relat. Area Mol. Biol*. **1988**, *61*, 381−436.

(14) Chen, Q. X.; Zhang, Z.; Zhou, X. W.; Zhuang, Z. L. Kinetics of inhibition of β-glucosidase from *Ampullarium crossean* by bromoacetic acid. *Int. J. Biochem. Cell Biol*. **2000**, *32*, 717−723.

(15) Zhou, X. W.; Zhuang, Z. L.; Chen, Q. X. Kinetics of inhibition of green crab (*Scylla serrata*) alkaline phosphatase by sodium (2,2″-bipyridine) oxodiperoxovanadate. *J. Protein Chem*. **1999**, *18*, 735−740.

(16) Zhang, R. Q.; Chen, Q. X.; Xiao, R.; Xie, L. P.; Zeng, X. G.; Zhou, H. M. Kinetics of inhibition of green crab (*Scylla serrata*) alkaline phosphatase by zinc ions: A new type of complexing inhibition. *Biochim. Biophys. Acta* **2001**, *1545*, 6−12.

(17) Chen, Q. X.; Zheng, W. Z.; Lin, J. Y.; Cai, Z. T.; Zhou, H. M. Kinetics of inhibition of green crab (*Scylla serrata*) alkaline phosphatase by vanadate. *Biochemistry (Moscow)* **2000**, *65*, 1305−1310.

(18) Himmelwright, R. S.; Eickman, N. C.; LuBien, C. D.; Lerch, K.; Solomon, E. I. Chemical and spectroscopic studies of the binuclear copper active site of *Newrospora* tyrosinase: Comparison of hemocyanin. *J. Am. Chem. Soc*. **1980**, *102*, 7339−7344.

(19) Solomon, E. I. In *Copper Proteins*; Spiro, T. G., Ed.; John Wiley and Sons: New York, 1981; pp 42−108.

(20) Wilcox, D. E.; Porras, A. G.; Hwang, Y. T.; Lerch, K.; Winkler, M. E.; Solomon, E. I. Substrate analogue binding to the coupled binuclear copper active site in tyrosinase. *J. Am. Chem. Soc*. **1985**, *107*, 4015−4027.

Received for review October 16, 2001. Revised manuscript received April 4, 2002. Accepted April 17, 2002. Q. X. C. thanks the Lee Foundation and the Berkeley Scholars Program for financial support during his study at the University of California, Berkeley.

JF011378Z